

Precision Electroweak Physics¹

Jens Erler

Instituto de Física, Universidad Nacional Autónoma de México, 04510 México D.F., México

Abstract. The status in electroweak precision physics is reviewed. I present a brief summary of the latest data, global fit results, a few implications for new physics, and an outlook.

OBSERVABLES

Z pole

The Z factories, LEP and SLC, have performed benchmark precision measurements for the electroweak Standard Model (SM) [1]. LEP scanned the Z lineshape yielding the Z boson mass, M_Z , with 2×10^{-5} relative precision, as well as its total width, Γ_Z , and hadronic peak cross section, $\sigma_{\text{had}}^0 \equiv 12\pi\Gamma(e^+e^-)\Gamma(\text{had})/M_Z^2\Gamma_Z^2$, both to better than one per mille accuracy. $\Gamma(\bar{f}f)$ is the Z partial decay width into fermion f and $\Gamma(\text{had})$ is the hadronic Z decay width. Results on the three leptonic ($\ell = e, \mu, \tau$) branching ratios, $R_\ell \equiv \Gamma(\text{had})/\Gamma(\ell^+\ell^-)$, are also at the per mille level. Γ_Z , σ_{had}^0 , and the R_ℓ are unique in their sensitivity to the strong coupling constant, α_s , which can be extracted with very small theoretical uncertainty. The SLC was able to compensate its lower luminosity by its electron beam polarization. The left-right polarization asymmetry, A_{LR} , for hadronic final states provides the currently most precise value of the weak mixing angle,

$$\sin^2 \theta_W = \frac{g'^2}{g^2 + g'^2}, \quad (1)$$

where g and g' are the $SU(2)_L$ and $U(1)_Y$ gauge couplings, respectively. Very high precision could also be achieved in the heavy flavor sector consisting of branching ratios and various asymmetries for b and c quarks. More specifically, the forward-backward (FB) asymmetry into b quarks, A_{FB}^b , amounts to the most precise measurement of $\sin^2 \theta_W$ at LEP, while the few per mille measurement of $R_b = \Gamma(\bar{b}b)/\Gamma(\text{had})$ yields independent information on the top quark mass, m_t , and constraints on new physics affecting the third generation in a non-universal way. The heavy flavor results have been finalized very recently. Analogous results are also available for s quarks, albeit with larger uncertainties. Other Z pole observables include the three leptonic FB asymmetries, A_{FB}^ℓ , the final state τ polarization and its FB asymmetry, and charge asymmetry measurements.

¹ Presented at the X Mexican Workshop on Particles and Fields, Morelia, Mich., November 6–12, 2005.

TABLE 1. Z pole observables compared with the SM best fit predictions. \bar{s}_ℓ^2 is an effective mixing angle which absorbs all radiative corrections and corresponds most closely to what enters the Z pole asymmetries. The first is extracted from the hadronic charge asymmetry, a weighted average over light-quark FB asymmetries. The second is from the final state electron FB asymmetry, A_{FB} , from CDF [2]. The three values of A_e are (i) from A_{LR} for hadronic final states [3]; (ii) from A_{LR} for leptonic final states and from polarized Bhabba scattering [4]; and (iii) from the angular distribution of the τ polarization (LEP) [1]. The two A_τ values are from SLD and the total τ polarization, respectively. The uncertainties in the SM predictions are induced by the errors in the SM parameters, and their correlations have been accounted for.

observable	experimental value	SM prediction	pull
M_Z [GeV]	91.1876 ± 0.0021	91.1874 ± 0.0021	0.1
Γ_Z [GeV]	2.4952 ± 0.0023	2.4968 ± 0.0011	-0.7
σ_{had}^0 [nb]	41.541 ± 0.037	41.467 ± 0.009	2.0
R_e	20.804 ± 0.050	20.756 ± 0.011	1.0
R_μ	20.785 ± 0.033	20.756 ± 0.011	0.9
R_τ	20.764 ± 0.045	20.801 ± 0.011	-0.8
R_b	0.21629 ± 0.00066	0.21578 ± 0.00010	0.8
R_c	0.1721 ± 0.0030	0.17230 ± 0.00004	-0.1
A_{FB}^e	0.0145 ± 0.0025	0.01622 ± 0.00025	-0.7
A_{FB}^μ	0.0169 ± 0.0013		0.5
A_{FB}^τ	0.0188 ± 0.0017		1.5
A_{FB}^b	0.0992 ± 0.0016	0.1031 ± 0.0008	-2.4
A_{FB}^c	0.0707 ± 0.0035	0.0737 ± 0.0006	-0.8
A_{FB}^s	0.0976 ± 0.0114	0.1032 ± 0.0008	-0.5
\bar{s}_ℓ^2	0.2324 ± 0.0012	0.23152 ± 0.00014	0.7
	0.2238 ± 0.0050		-1.5
A_e	0.15138 ± 0.00216	0.1471 ± 0.0011	2.0
	0.1544 ± 0.0060		1.2
	0.1498 ± 0.0049		0.6
A_μ	0.142 ± 0.015		-0.3
A_τ	0.136 ± 0.015		-0.7
	0.1439 ± 0.0043		-0.7
A_b	0.923 ± 0.020	0.9347 ± 0.0001	-0.6
A_c	0.670 ± 0.027	0.6678 ± 0.0005	0.1
A_s	0.895 ± 0.091	0.9356 ± 0.0001	-0.4

These Z pole measurements are summarized in Table 1. Some results are quoted in terms of asymmetry parameters,

$$A_f \equiv \frac{2v_f a_f}{v_f^2 + a_f^2}, \quad (2)$$

where at tree level the $Zf\bar{f}$ vector (axial-vector) coupling is given by $v_f = T_3^f - 2Q^f \sin^2 \theta_W$ ($a_f = T_3^f$), and where Q^f and T^f denote, respectively, the electric charge and third component of weak isospin of fermion f . The FB asymmetries can also be expressed in terms of these, $A_{FB}^f = 3/4 A_e A_f$.

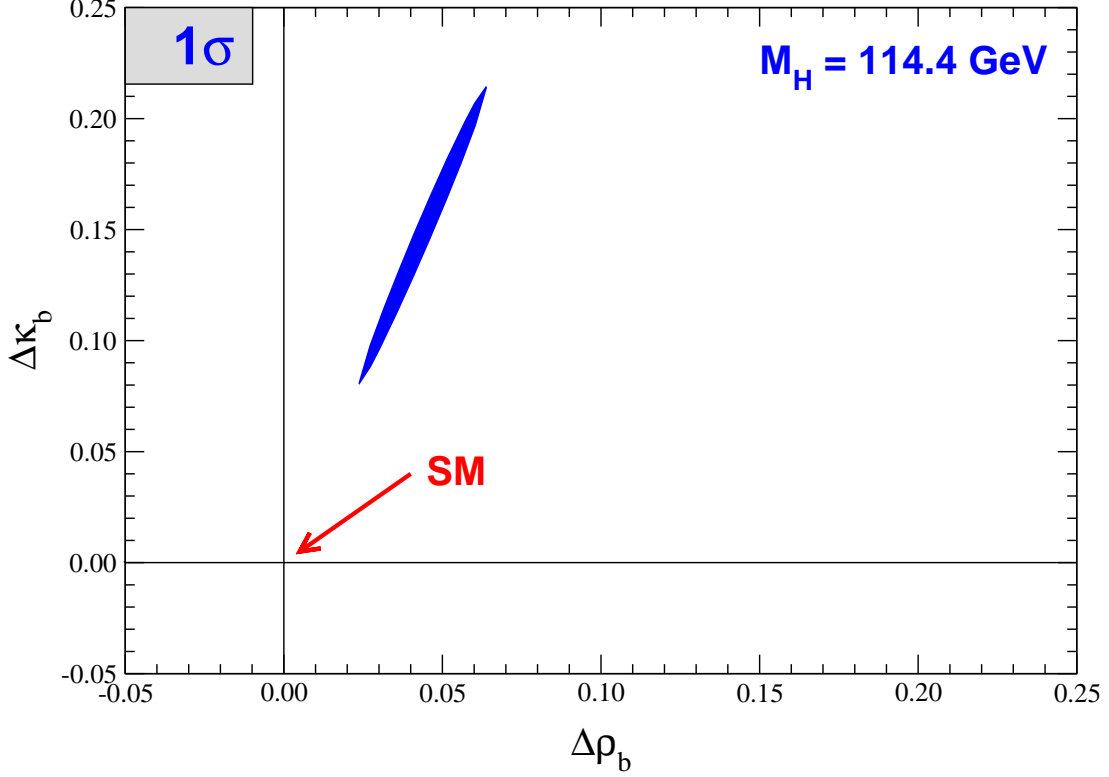


FIGURE 1. New Physics contributions to form factors for the $Zb\bar{b}$ vector and axial-vector couplings.

The pull of an observable gives its deviation from the SM and is defined as,

$$\text{pull}(O_i) = \frac{O_i^{\text{exp.}} - O_i^{\text{SM}}}{\Delta O_i^{\text{total}}}, \quad (3)$$

where $O_i^{\text{exp.}}$ is the experimental central value of observable, O_i , O_i^{SM} is the central value of its SM prediction, and $\Delta O_i^{\text{total}}$ is the sum in quadrature of the contributing statistical, systematical, and theoretical uncertainties, but excludes the parametric uncertainty in the SM prediction. As can be seen from Table 1, there are only three Z pole observables which deviate by two standard deviations (σ) or more, but interestingly these are all among the most precise. In particular, A_{LR} and A_{FB}^b provide valuable information on the mass of the Higgs boson, M_H , and deviate by 3.1σ from each other. Since A_{FB}^b involves b quarks, and the third fermion generation is often suspected to be affected differently by physics beyond the SM, one can interpret it alternatively as a measurement of $Zb\bar{b}$ couplings. Defining,

$$\begin{aligned} v_b &= (1 + \Delta\hat{\rho}_b + \Delta\rho_b)[T_3^f - 2Q^f(1 + \Delta\hat{\kappa}_b + \Delta\kappa_b)\sin^2\theta_W], \\ a_b &= (1 + \Delta\hat{\rho}_b + \Delta\rho_b)T_3^f, \end{aligned} \quad (4)$$

one can fit to $\Delta\rho_b$ and $\Delta\kappa_b$, which are due to new physics only when all SM contributions are subsumed in $\Delta\hat{\rho}_b$ and $\Delta\hat{\kappa}_b$. R_b and A_b provide additional constraints. The result is

shown in Fig. 1, from where it becomes clear that a correction of 10–20% to $\Delta\kappa_b$ would be necessary to account for the data. This would be a very large radiative correction, given that the quadratically enhanced top quark contribution in the SM is less than 1%. It is thus very unlikely that the deviation in A_{FB}^b is due to a loop effect, but it is conceivably of tree-level type affecting preferentially the third generation. Examples include the decay of a scalar neutrino resonance [5], mixing of the b quark with heavy exotics [6], and a heavy Z' with family non-universal couplings [7]. It is difficult, however, to simultaneously account for R_b , which has been measured on the Z peak and off-peak [1] at LEP 1. In this context it is interesting that an average of R_b measurements at LEP 2 at energies between 133 and 207 GeV is 2.1σ below the SM prediction, and A_{FB}^b is 1.6σ low [8].

The measurement of σ_{had}^0 is 2σ higher than the SM prediction. As a consequence, when one fits to the number, N_ν , of active neutrinos² one obtains a 2σ deficit, $N_\nu = 2.986 \pm 0.007$, compared to the SM prediction, $N_\nu = 3$. Amusingly, LEP 2 [8] also sees a 1.7σ excess in the averaged hadronic cross section.

Other data

Table 2 lists non- Z pole observables. Precise values for the W boson mass, M_W , have been obtained at the high energy frontier at LEP 2 [8] (e^+e^-) and the Tevatron [10, 11] ($p\bar{p}$). The world average, $M_W = 80.410 \pm 0.032$ GeV, has reached a relative precision of 4×10^{-4} with further improvements expected in the near future. The direct measurements [23] of $m_t = 172.7 \pm 2.9 \pm 0.6$ GeV from the Tevatron³ can be compared to an indirect determination, $m_t = 172.3_{-7.6}^{+10.2}$ GeV, from the other precision data. The agreement is spectacular. As shown in Fig. 2, this comparison can even be carried out for the two parameters, m_t and M_W , simultaneously. In the indirect determination, m_t is mostly constrained by R_b , but Γ_Z and low energy measurements also contribute significantly. M_W is then mostly implied by the asymmetries. The agreement is again remarkable and it should be stressed that there are now two theoretically and experimentally independent indications for a relatively light Higgs boson with a mass of $\mathcal{O}(100 \text{ GeV})$. The implications of various sets of observables for M_H and m_t are shown in Fig. 3.

Other important measurements are from comparatively lower energies or momentum transfers [24]. The most precise are determinations of anomalous magnetic moments in leptons, a_ℓ . The measurement [25] of a_μ stands out because of its unique sensitivity to high energy scales. If the new physics [26] couples, respectively, through tree or one-loop effects, a simple dimensional estimate of the scales that can be probed by a_μ at the 1σ level (Δa_μ denotes the total error) gives,

$$\Lambda_{\text{new}} \sim \frac{m_\mu}{\sqrt{\Delta a_\mu}} \sim 3.7 \text{ TeV}, \quad \frac{\Lambda_{\text{new}}}{g} \sim \frac{1}{2\pi} \frac{m_\mu}{\sqrt{\Delta a_\mu}} \sim 590 \text{ GeV}. \quad (5)$$

² By definition, an active neutrino is one that couples to the Z boson like a standard neutrino.

³ The first error is experimental [23] and the second is theoretical from the conversion from the top pole mass to the $\overline{\text{MS}}$ mass, the quantity which actually enters the radiative corrections.

TABLE 2. Non-Z pole observables compared with the SM best fit predictions. The first M_W value is from UA2 [9], CDF [10], and DØ [11], and the second is from LEP 2 [8]. g_L^2 and g_R^2 (see text) are from NuTeV [12], while the older neutrino deep-inelastic scattering (ν -DIS) results from CDHS [13], CHARM [14], and CCFR [15] are included in the fits, but not shown. $g_{V,A}^{ve}$ are world averaged effective four-Fermi couplings in νe scattering and dominated by the CHARM II results [16]. A_{PV} is the parity violating asymmetry in Møller scattering [17]. $Q_W(\text{Cs})$ [18, 19] and $Q_W(\text{Tl})$ [20, 21] are the so-called weak charges of Cs and Tl and have been determined in atomic parity violation (APV) experiments. The APV errors shown contain significant theory uncertainties from atomic structure calculations [22]. In the case of τ_τ (see text) the theory uncertainty is included in the SM prediction. In all other SM predictions, the uncertainty is from the SM parameters.

observable	experimental value	SM prediction	pull
m_t [GeV]	172.7 ± 3.0	172.7 ± 2.8	0.0
M_W [GeV]	80.450 ± 0.058	80.376 ± 0.017	1.3
	80.392 ± 0.039		0.4
g_L^2	0.30005 ± 0.00137	0.30378 ± 0.00021	-2.7
g_R^2	0.03076 ± 0.00110	0.03006 ± 0.00003	0.6
g_V^{ve}	-0.040 ± 0.015	-0.0396 ± 0.0003	0.0
g_A^{ve}	-0.507 ± 0.014	-0.5064 ± 0.0001	0.0
A_{PV}	-1.31 ± 0.17	-1.53 ± 0.02	1.3
$Q_W(\text{Cs})$	-72.62 ± 0.46	-73.17 ± 0.03	1.2
$Q_W(\text{Tl})$	-116.6 ± 3.7	-116.78 ± 0.05	0.1
$a_\mu - \frac{\alpha}{2\pi}$	4511.07 ± 0.82	4509.82 ± 0.10	1.5
τ_τ [fs]	290.89 ± 0.58	291.87 ± 1.76	-0.4

The interpretation of a_μ is complicated by hadronic contributions which first arise at the two-loop level. One can use experimental $e^+e^- \rightarrow \text{hadrons}$ cross section data to estimate [27] the two-loop effect, which is due to a vacuum polarization (VP) insertion into a one-loop graph, $a_\mu^{(2,\text{VP})} = (69.54 \pm 0.64) \times 10^{-9}$. This value suggests a 2.3 σ discrepancy between the SM and experiment. If one assumes isospin symmetry (which is not exact and appropriate corrections [28] have to be applied) one can also make use of τ decay spectral functions [29] and one obtains [30], $a_\mu^{(2,\text{VP})} = (71.10 \pm 0.58) \times 10^{-9}$. This result implies no conflict (0.7 σ) between data and prediction. It is important to understand the origin of this difference, but the following observations point to the conclusion that at least some of it is experimental: (i) The latest e^+e^- data by the SND Collaboration [31] are consistent with the implications of the τ decay data, and in conflict with other e^+e^- data. (ii) The $\tau^- \rightarrow \nu_\tau 2\pi^- \pi^+ \pi^0$ spectral function disagrees with the corresponding e^+e^- data at the 4 σ level, which translates to a 23% effect [27] and seems too large to arise from isospin violation. (iii) Isospin violating corrections have been studied in detail in Ref. [28] and found to be largely under control. The largest effect is due to higher-order electroweak corrections [32] but introduces a negligible uncertainty [33]. (iv) Ref. [34] shows on the basis of a QCD sum rule that the spectral functions derived from τ decay data are consistent with values of $\alpha_s(M_Z) \gtrsim 0.120$ (in agreement with the global fit result described in the next section), while the spectral

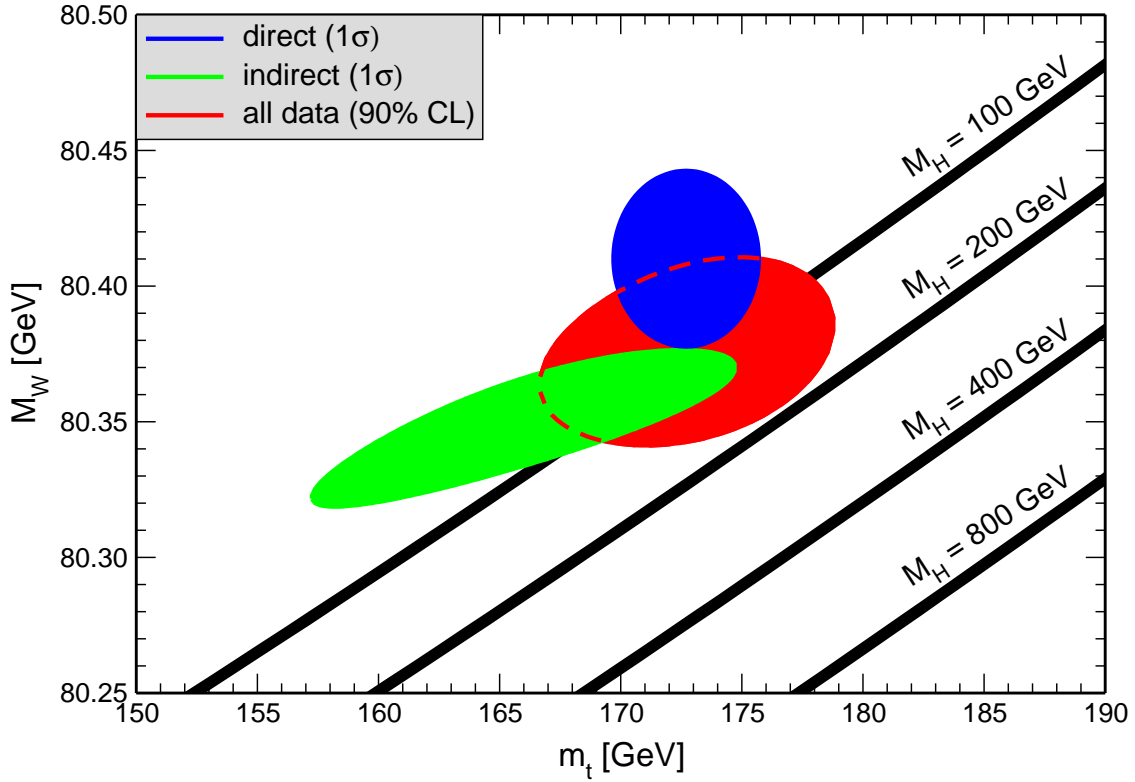


FIGURE 2. One-standard-deviation (39.35%) region in M_W as a function of m_t for the direct and indirect data, and the 90% CL region ($\Delta\chi^2 = 4.605$) allowed by all data. The SM prediction as a function of M_H is also indicated. The width of the M_H bands reflects the theoretical uncertainty in the prediction.

functions from e^+e^- annihilation are consistent only for somewhat lower (disfavored) values. In any case, due to the suppression at large momentum transfer (from where the conflicts originate) these problems are less pronounced as far as $a_\mu^{(2,VP)}$ is concerned, so that it seems justified to view these differences as fluctuations and to average the results. An additional uncertainty is induced by the hadronic three-loop light-by-light scattering contribution. For this the most recent value, $a_\mu^{\text{LBLS}} = (1.36 \pm 0.25) \times 10^{-9}$, of Ref. [35] is employed, which is higher than previous evaluations [36, 37].

The τ is the only lepton which can decay hadronically, offering a luxurious arena to study the strong interaction and to extract α_s . Its mass, m_τ , is large enough that the operator product expansion, OPE (QCD perturbation theory plus almost negligible power corrections in an expansion in the inverse τ mass), can be applied, yet small enough that QCD effects are sizable with great sensitivity to α_s . Upon renormalization group evolution from m_τ to M_Z (where α_s can be compared to the values from Γ_Z , σ_{had}^0 , and R_ℓ), the uncertainty scales roughly⁴ like $\alpha_s(M_Z)^2/\alpha_s(m_\tau)^2 \sim 0.12$. Furthermore, because the

⁴ This order of magnitude decrease is sometimes called the “incredibly shrinking error”.

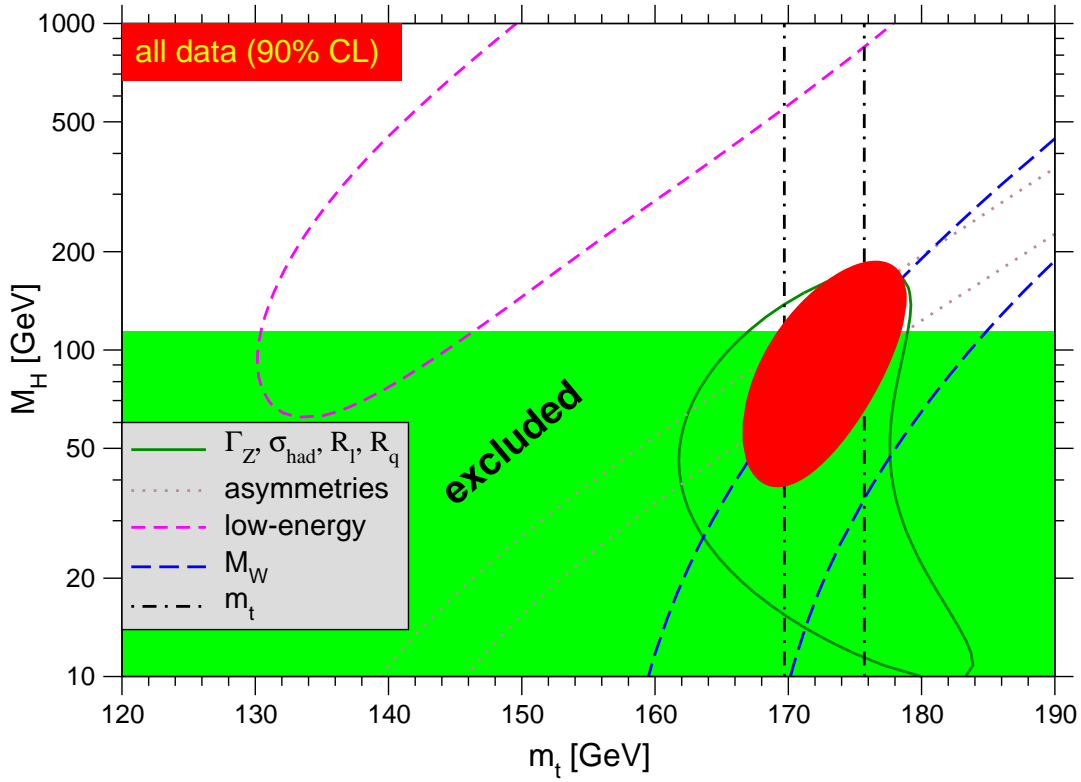


FIGURE 3. One-standard-deviation (39.35%) uncertainties in M_H as a function of m_t for various inputs, and the 90% CL region allowed by all data. $\alpha_s(M_Z) = 0.120$ is assumed except for the fits including the Z lineshape data. The 95% direct lower limit from LEP 2 is also shown.

τ lifetime, τ_τ , and leptonic branching ratios⁵ are fully inclusive, there are no uncertainties from hadronization, fragmentation, parton distribution functions, or other modeling of the strong interaction. The only potential theoretical uncertainties are from the truncation of the perturbative series and from non-perturbative OPE breaking effects. The perturbative series is known up to $\mathcal{O}(\alpha_s^3)$ (the same order as the QCD correction to $\Gamma(\text{had})$) and should therefore not be combined with only next-to-leading order determinations of α_s . The coefficients that enter the α_s expansion of τ_τ are relatively large, but dominated by terms that arise from analytical continuation and are thus proportional to QCD β -function coefficients. Since the latter are known to $\mathcal{O}(\alpha_s^4)$ and first enter at $\mathcal{O}(\alpha_s^2)$, it is advantageous to treat these effects separately and re-sum them to all orders. This amounts to a re-organization of the perturbative series (also referred to as “contour improvement”) with smaller expansion coefficients⁶ and where α_s^n is replaced by more complicated functions, $A_n(\alpha_s)$. The dominant uncertainty is from the lack of knowledge of the four-loop coefficient, d_3 . One is still exposed to OPE breaking non-perturbative

⁵ The τ lifetime world average in Table 2 is computed by combining the direct measurements with values derived from the leptonic branching ratios.

⁶ These coefficients are given by those of the Adler D -function, d_i .

effects because at one kinematic point one needs to change from quark degrees of freedom (QCD) to hadrons (data), but fortunately this point is suppressed by a double zero. Very precise data on τ spectral functions (mainly from ALEPH [29]) constrain such effects to a sub-dominant level.

Currently the largest discrepancy is from ν -DIS scattering. The NuTeV Collaboration finds for the on-shell definition of the weak mixing angle, $s_W^2 = 0.2277 \pm 0.0016$, which is 3.0σ higher than the SM prediction. The discrepancy is in the left-handed effective four-Fermi coupling, $g_L^2 = 0.3000 \pm 0.0014$, which is 2.7σ low, while $g_R^2 = 0.0308 \pm 0.0011$ is 0.6σ high. At tree level, these are given by,

$$g_L^2 \approx \frac{1}{2} - \sin^2 \theta_W + \frac{5}{9} \sin^4 \theta_W, \quad g_R^2 \approx \frac{5}{9} \sin^4 \theta_W. \quad (6)$$

Within the SM, one can identify five categories of effects that could cause or contribute to this effect [38]: (i) an asymmetric strange quark sea, although this possibility is constrained by dimuon data [39]; (ii) isospin symmetry violating parton distribution functions at levels much stronger than generally expected [40]; (iii) nuclear physics effects [41, 42]; (iv) QED and electroweak radiative corrections [43, 44]; and (v) QCD corrections to the structure functions [45]. The NuTeV result and the other ν -DIS data should therefore be considered as preliminary until a re-analysis using PDFs including all experimental and theoretical information has been completed. It is well conceivable that various effects add up to bring the NuTeV result in line with the SM prediction. It is likely that the overall uncertainties in g_L^2 and g_R^2 will increase, but at the same time the older ν -DIS results may become more precise when analyzed with better PDFs than were available at the time.

GLOBAL FIT

With these inputs a simultaneous fit to various SM parameters can be performed,

$$\begin{aligned} M_Z &= 91.1874 \pm 0.0021 \text{ GeV}, \\ M_H &= 89_{-28}^{+38} \text{ GeV}, \\ m_t &= 172.7 \pm 2.8 \text{ GeV}, \\ \alpha_s(M_Z) &= 0.1216 \pm 0.0017, \\ \hat{\alpha}(M_Z)^{-1} &= 127.904 \pm 0.019, \\ \sin^2 \hat{\theta}_W &= 0.23122 \pm 0.00015, \\ s_W^2 \equiv 1 - \frac{M_W^2}{M_Z^2} &= 0.22306 \pm 0.00033, \end{aligned} \quad (7)$$

where the last two lines show the weak mixing angle in the $\overline{\text{MS}}$ -scheme (coupling based) and the on-shell scheme (vector meson mass based), respectively. $\hat{\alpha}(M_Z)$ is the $\overline{\text{MS}}$ electromagnetic coupling as it enters at the Z pole. Despite the small discrepancies discussed in the previous section, the goodness of the fit to all data is very good with a $\chi^2/\text{d.o.f.} = 47.5/42$. The probability of a larger χ^2 is 26%. Experimental correlations have been taken into account. Theoretical correlations, *e.g.* between $\hat{\alpha}(M_Z)$ and $g_\mu - 2$

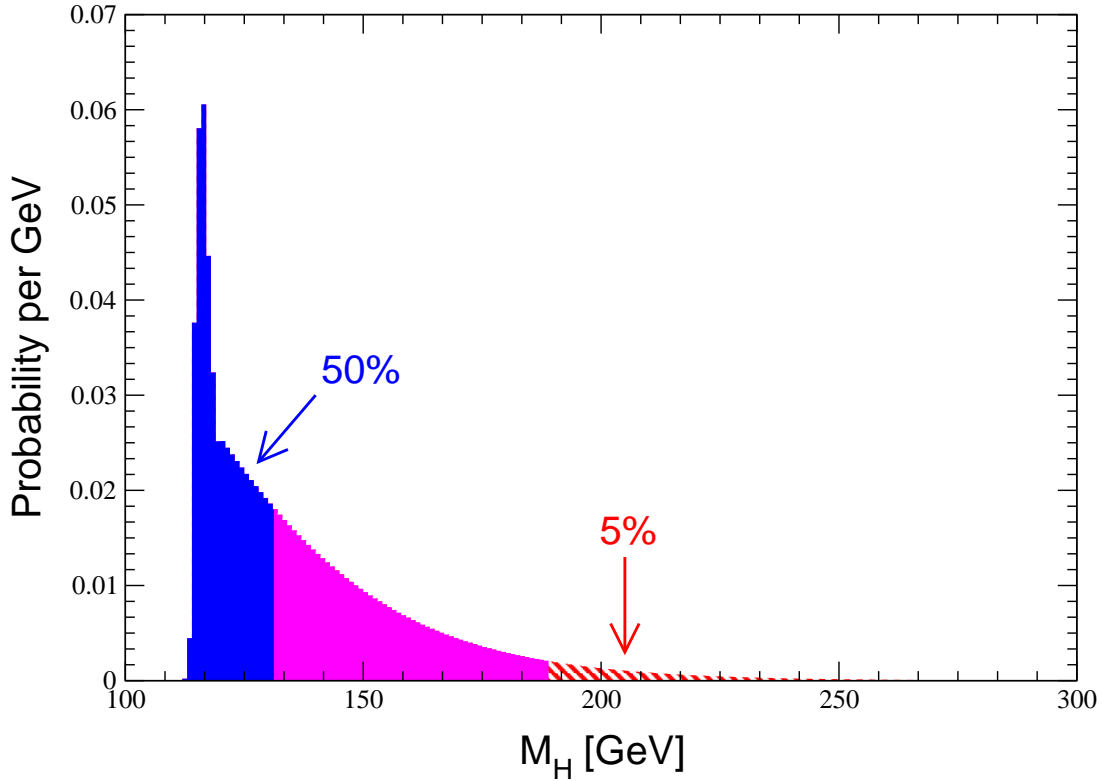


FIGURE 4. Probability distribution function of M_H including direct search results.

are also addressed⁷. The measurement of the latter is higher than the SM prediction, and its inclusion in the fits favors a larger $\hat{\alpha}(M_Z)$ and a lower M_H by about 3 GeV.

The extracted Z pole value of $\alpha_s(M_Z)$ is based on a formula with almost negligible theoretical uncertainty (± 0.0005 in $\alpha_s(M_Z)$) if one assumes the exact validity of the SM. One should keep in mind, however, that this value⁸, $\alpha_s = 0.1198 \pm 0.0028$, is very sensitive to such types of new physics as non-universal vertex corrections. In contrast, the value derived from τ decays, $\alpha_s(M_Z) = 0.1225^{+0.0025}_{-0.0022}$, is theory dominated but less sensitive to new physics. The two values are in remarkable agreement with each other. They are also in good agreement with other recent values, such as from a 4-jet analysis at OPAL [46] (0.1182 ± 0.0026) and from jet production at HERA [47] (0.1186 ± 0.0051), but the τ decay result is somewhat higher than the value, 0.1170 ± 0.0012 , from the most recent unquenched lattice calculation [48].

There is a strong correlation between the quadratic m_t and logarithmic M_H terms in the radiative corrections except for the $Z \rightarrow b\bar{b}$ -vertex. M_W has additional M_H dependence

⁷ This is due to the common use of the experimental $e^+e^- \rightarrow$ hadrons cross section and τ decay data. The weak mixing angle for momentum transfers at or below hadronic scales and various hadronic three-loop contributions to a_μ need these inputs, as well, implying additional correlations.

⁸ If one adds non- Z pole observables (other than τ_τ or τ leptonic branching ratios), one obtains the slightly higher value, $\alpha_s = 0.1202 \pm 0.0027$.

which is not coupled to m_t^2 effects. The strongest individual pulls toward smaller M_H are from M_W and A_{LR} (SLD), while A_{FB}^b and the NuTeV results favor higher values. The difference in χ^2 for the global fit is, $\Delta\chi^2 = \chi^2(M_H = 1000 \text{ GeV}) - \chi_{\min}^2 = 60$. Hence, the data clearly favor a small value of M_H , as in supersymmetric extensions of the SM. The 90% central confidence range from all precision data is $46 \text{ GeV} \leq M_H \leq 154 \text{ GeV}$. The central value of the global fit result, $M_H = 89_{-28}^{+38} \text{ GeV}$, is below the direct LEP 2 lower bound, $M_H \geq 114.4 \text{ GeV}$ (95% CL) [49]. Including the results of these direct searches as an extra contribution to the likelihood function drives the 95% upper limit to $M_H \leq 189 \text{ GeV}$. As two further refinements, the theoretical uncertainties from uncalculated higher order contributions and the M_H -dependence of the correlation matrix which gives slightly more weight to lower Higgs masses [50] are accounted for. The resulting limits at 95 (90, 99)% CL are

$$M_H \leq 194 (176, 235) \text{ GeV}, \quad (8)$$

respectively. The probability distribution function of M_H is shown in Fig. 4.

NEW PHYSICS AND OUTLOOK

The good agreement between SM predictions and experiments implies strong constraints on new physics scenarios beyond the SM. The Z pole measurements are particularly suitable to study possible new physics effects on the Z couplings to quarks and leptons. The per mille precision which has been achieved at LEP and SLC allows, for example, only very small mixing between the Z and a hypothetical extra Z' boson [51]. On the other hand, a Z' with no or little mixing, or other types of new physics contributing to e^+e^- amplitudes without affecting Z boson properties, could have easily gone unnoticed, since such effects may hide under the Z resonance. It is then expedient to examine precision observables away from the Z pole. High quality and high energy data are provided by LEP 2 [8], although these come with comparatively low rates. An interesting alternative is to utilize low energy observables probing directly the weak interaction. This includes processes which exploit the parity violating character of the weak interaction, as well as neutrino scattering.

For example, the E158 Collaboration at SLAC [17] has extracted the weak charge of the electron, $Q_W(e)$, from the parity violating asymmetry, A_{PV} , in polarized electron scattering, $\vec{e}e$. A 13% error in the Møller asymmetry suffices to access the TeV scale. A similar experiment, Qweak at JLab [52], will determine the analogous proton weak charge, $Q_W(p)$, in $\vec{e}p$ -scattering. The new physics scales probed by $Q_W(e)$ [53] and $Q_W(p)$ [54] reach (at the 1σ level),

$$\frac{\Lambda_{\text{NEW}}}{g} \approx \frac{1}{\sqrt{\sqrt{2}G_F|\Delta Q_W|}} \approx \begin{cases} 4.6 \text{ TeV } [Q_W(p)], \\ 3.2 \text{ TeV } [Q_W(e)], \end{cases} \quad (9)$$

where g is the coupling strength of the new physics, G_F is the Fermi constant, and $|\Delta Q_W|$ is the total uncertainty (a 4% determination of $Q_W(p)$ is assumed). The reason for the high reach in these experiments is a suppression of the tree-level SM contribution which is proportional to $1 - 4 \sin^2 \theta_W$. The numerical value of $\sin^2 \theta_W$ which enters at very low

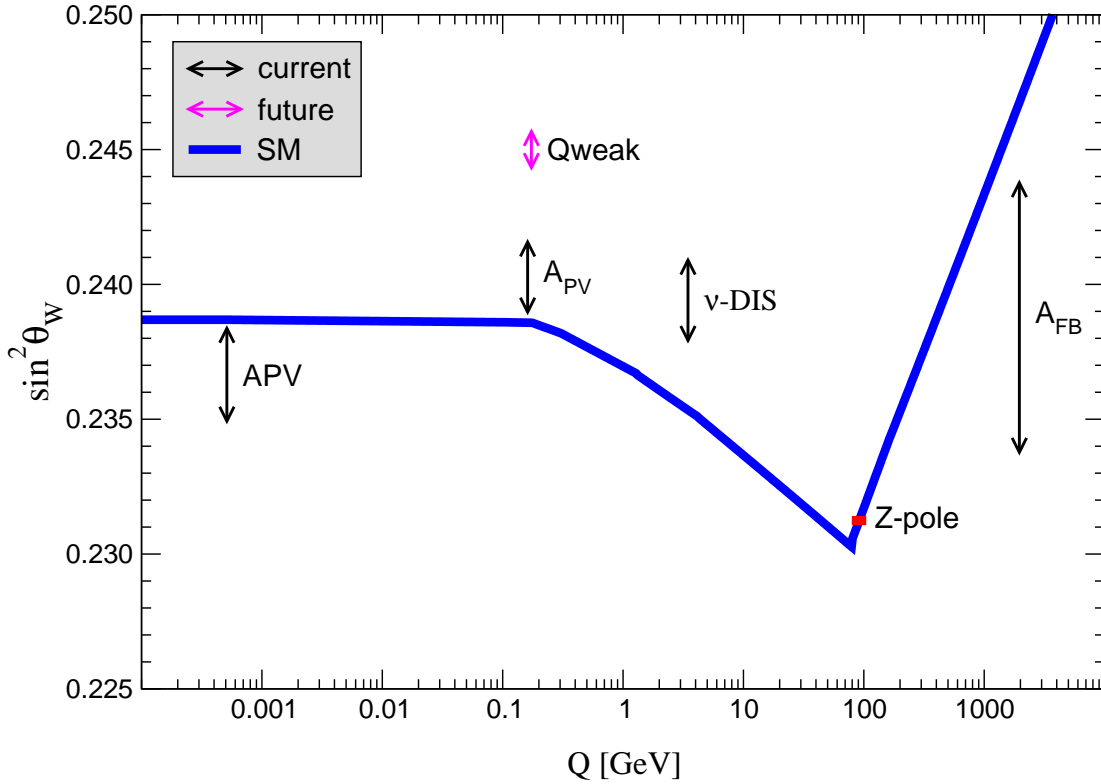


FIGURE 5. The weak mixing angle in the $\overline{\text{MS}}$ -scheme as a function of energy, $\sqrt{Q^2}$. The width of the line indicates the uncertainty in the SM prediction. The mixing angle can be determined from a variety of neutral-current processes spanning a very wide Q^2 range. The largest discrepancy is the measurement from ν -DIS which is 2.7σ above the prediction. This is mostly due to the NuTeV result [12]. The figure is updated from Ref. [55].

momentum transfer ($Q^2 \approx 0.03 \text{ GeV}^2$ in these experiments) is even closer to the ideal value of $1/4$ than the one entering Z pole physics ($Q^2 = M_Z^2$). This is illustrated in Fig. 5.

This kind of low energy, very high statistics measurement may even compete with the Z factories. For example, a factor of 4 improvement in A_{PV} relative to the E158 result (which can conceivably be achieved at an upgraded 12 GeV CEBAF at JLab) would yield a measurement of the low energy mixing angle to about ± 0.00035 . Fig. 6 shows a breakdown of our current knowledge of the weak mixing angle. A possible projection into the intermediate future is also shown, where a 3.25% A_{PV} and a 4% $Q_W(p)$ measurement are assumed, along with some expected improvements [56] at the Tevatron Run IIA (corresponding approximately to an accumulated luminosity of 2 fb^{-1} of data). It is entertaining to also display what such an outcome would mean for the various laboratories. Fig. 7 shows that JLab with a dedicated asymmetry physics program could contribute almost as much to $\sin^2 \theta_W$ as the high-energy laboratories, SLAC and FNAL.

One can also consider the general effects on neutral-current and Z and W boson observables of various types of heavy new physics which contribute to the W and Z self-energies but which do not have any (or only small) direct coupling to the ordi-

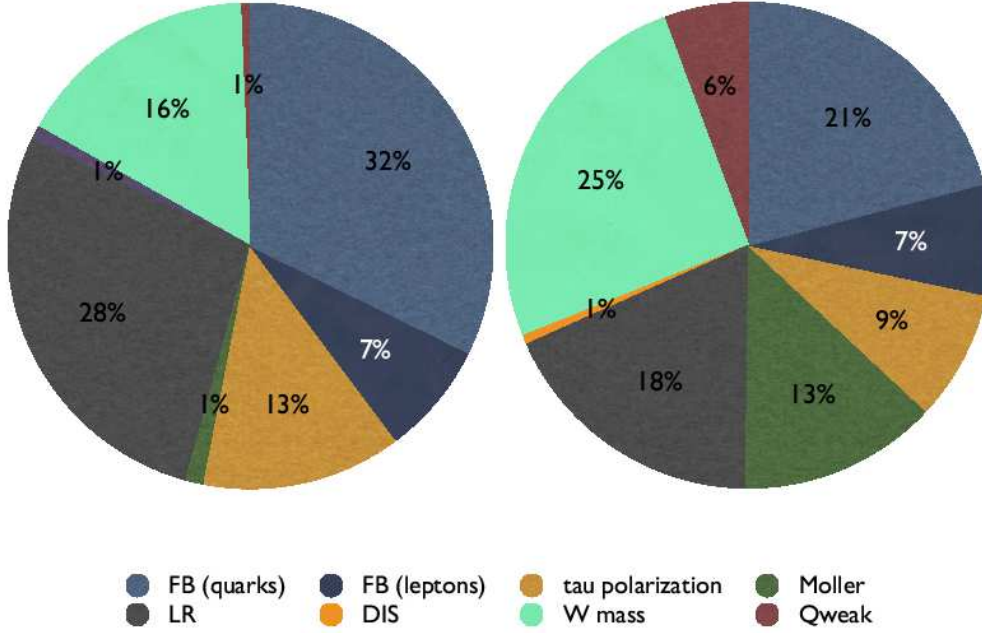


FIGURE 6. Precision weighted contributors to our knowledge of the weak mixing angle, $\sin^2 \theta_W$, by type of observable. The left-hand side is the status, while the right-hand side is a projection into the intermediate future, assuming 3.5% A_{PV} and 4% $Q_W(p)$ determinations, as well as 2 fb^{-1} of Tevatron Run IIA data. The W mass can be regarded as a measurement of the on-shell mixing angle, s_W^2 . Q_{weak} refers to the weak charges of the proton (Q_{weak}) and heavy nuclei (APV).

nary fermions. In addition to non-degenerate multiplets, which break the vector part of $SU(2)_L$, these include heavy degenerate multiplets of chiral fermions which break the axial generators. Such effects can be described by just three parameters, S , T , and U [57]. T is equivalent to the electroweak ρ -parameter [58] and proportional to the difference between the W and Z self-energies at $Q^2 = 0$ (vector $SU(2)_L$ -breaking). S and $S + U$ are associated, respectively, with the difference between the Z and W self-energies at $Q^2 = M_{Z,W}^2$ and $Q^2 = 0$ (axial $SU(2)_L$ -breaking). S , T , and U are defined with a factor proportional to $\hat{\alpha}$ removed, so that they are expected to be of order unity in the presence of new physics. A heavy non-degenerate multiplet of fermions or scalars contributes positively to T , while a multiplet of heavy degenerate chiral fermions increases S . For example, a heavy degenerate ordinary or mirror family would contribute $2/(3\pi)$ to S .

The data allow a simultaneous determination of S , T , U , and all SM parameters except for M_H ,

$$\begin{aligned}
 S &= -0.13 \pm 0.10 \text{ } (-0.08), \\
 T &= -0.13 \pm 0.11 \text{ } (+0.09), \\
 U &= 0.20 \pm 0.12 \text{ } (+0.01), \\
 \alpha_s(M_Z) &= 0.1223 \pm 0.0018,
 \end{aligned} \tag{10}$$

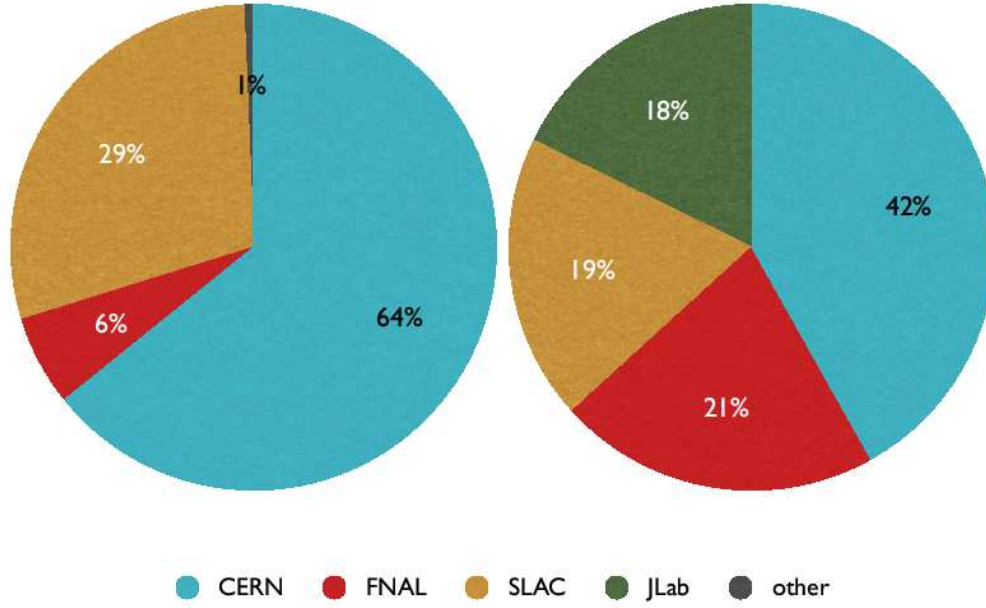


FIGURE 7. Contributors to our knowledge of the weak mixing angle, $\sin^2 \theta_W$, by laboratory. The left-hand side is the status, while the right-hand side is the projection using the same assumptions as in Fig 6.

where the uncertainties are from the inputs. The central values assume $M_H = 117$ GeV, and in parentheses the change for $M_H = 300$ GeV is shown. As can be seen, $\alpha_s(U)$ can be determined with no (little) M_H dependence. On the other hand, S , T , and M_H cannot be obtained simultaneously, because the Higgs boson loops themselves are resembled approximately by oblique effects. Eqs. (10) show that negative (positive) contributions to the S (T) parameter can weaken or entirely remove the strong constraints on M_H from the SM fits. The parameters in Eqs. (10), which by definition are due to new physics only, all deviate by more than one standard deviation from the SM values of zero. However, these deviations are correlated. Fixing $U = 0$ (as is done in Fig. 8) will also move S and T to values compatible with zero within errors. Note the strong correlation (84%) between the S and T parameters.

An extra generation of ordinary fermions is excluded at the 99.999% CL on the basis of the S parameter alone, corresponding to $N_F = 2.81 \pm 0.24$ for the number of families. This result assumes that there are no new contributions to T or U and therefore that any new families are degenerate. In principle this restriction can be relaxed by allowing T to vary as well, since $T > 0$ is expected from a non-degenerate extra family. However, the data currently favor $T < 0$, thus strengthening the exclusion limits. A more detailed analysis is required if the extra neutrino (or the extra down-type quark) is close to its direct mass limit [59, 60]. This can drive S to small or even negative values but at the expense of too-large contributions to T .

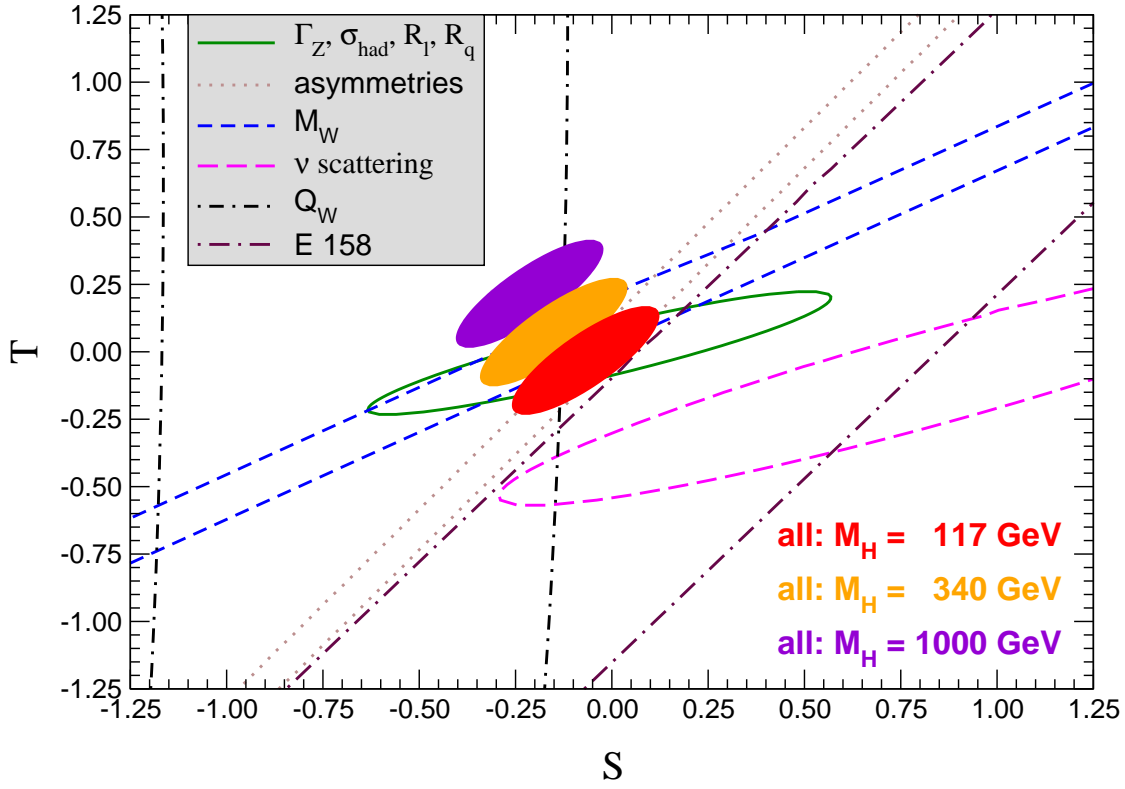


FIGURE 8. 1σ constraints on S and T from various inputs combined with M_Z . S and T represent the contributions of new physics only. The contours assume $M_H = 117$ GeV except for the central and upper 90% CL contours allowed by all data which are for $M_H = 340$ GeV and 1000 GeV, respectively. α_s is constrained using the τ lifetime as additional input in all fits.

ACKNOWLEDGMENTS

It is a pleasure to thank Paul Langacker and Michael Ramsey-Musolf for fruitful collaborations. This work was supported by CONACyT (México) contract 42026-F and by DGAPA-UNAM contract PAPIIT IN112902.

REFERENCES

1. ALEPH, DELPHI, L3, OPAL, and SLD Collaborations, LEP and SLD Electroweak Working Groups and SLD Heavy Flavour Group: S. Schael *et al.*, eprint hep-ex/0509008.
2. CDF Collaboration: D. Acosta *et al.*, *Phys. Rev.* **D71**, 052002 (2005).
3. SLD Collaboration; K. Abe *et al.*, *Phys. Rev. Lett.* **84**, 5945–5949 (2000).
4. SLD Collaboration; K. Abe *et al.*, *Phys. Rev. Lett.* **86**, 1162–1166 (2001).
5. J. Erler, J. L. Feng and N. Polonsky, *Phys. Rev. Lett.* **78**, 3063–3066 (1997).
6. D. Choudhury, T. M. P. Tait and C. E. M. Wagner, *Phys. Rev.* **D65**, 053002 (2002).
7. J. Erler and P. Langacker, *Phys. Rev. Lett.* **84**, 212–215 (2000).
8. ALEPH, DELPHI, L3, and OPAL Collaborations and LEP Electroweak Working Group: J. Alcaraz *et al.*, eprint hep-ex/0511027.
9. UA2 Collaboration: J. Alitti *et al.*, *Phys. Lett.* **B276**, 354–364 (1992).

10. CDF Collaboration: T. Affolder *et al.*, *Phys. Rev.* **D64**, 052001 (2001).
11. DØ Collaboration: V. M. Abazov *et al.*, *Phys. Rev.* **D66**, 012001 (2002).
12. NuTeV Collaboration: G. P. Zeller *et al.*, *Phys. Rev. Lett.* **88**, 091802 (2002).
13. CDHS Collaboration: H. Abramowicz *et al.*, *Phys. Rev. Lett.* **57**, 298–301 (1986).
14. CHARM Collaboration: J. V. Allaby *et al.*, *Phys. Lett.* **B177**, 446–452 (1986).
15. CCFR Collaboration: C. Arroyo *et al.*, *Phys. Rev. Lett.* **72**, 3452–3455 (1994).
16. CHARM-II Collaboration: P. Vilain *et al.*, *Phys. Lett.* **B335**, 246–252 (1994).
17. SLAC E158 Collaboration: P. L. Anthony *et al.*, *Phys. Rev. Lett.* **95**, 081601 (2005).
18. C. S. Wood *et al.*, *Science* **275**, 1759–1763 (1997).
19. J. Guena, M. Lintz and M. A. Bouchiat, eprint [physics/0412017](#).
20. N. H. Edwards, S. J. Phipp, P. E. G. Baird and S. Nakayama, *Phys. Rev. Lett.* **74**, 2654–2657 (1995).
21. P. A. Vetter *et al.*, *Phys. Rev. Lett.* **74**, 2658–2661 (1995).
22. J. S. M. Ginges and V. V. Flambaum, *Phys. Rep.* **397**, 63–154 (2004).
23. CDF and DØ Collaborations and Tevatron Electroweak Working Group: J. F. Arguin *et al.*, eprint [hep-ex/0507091](#).
24. For a review, see J. Erler and M. J. Ramsey-Musolf, *Prog. Part. Nucl. Phys.* **54**, 351–442 (2005).
25. Muon g-2 Collaboration: G. W. Bennett *et al.*, *Phys. Rev. Lett.* **92**, 161802 (2004).
26. For a review, see A. Czarnecki and W. J. Marciano, *Phys. Rev.* **D64**, 013014 (2001).
27. M. Davier, A. Höcker and Z. Zhang, eprint [hep-ph/0507078](#).
28. V. Cirigliano, G. Ecker and H. Neufeld, *JHEP* **0208**, 002 (2002).
29. ALEPH Collaboration: S. Schael *et al.*, *Phys. Rep.* **421**, 191–284 (2005).
30. M. Davier, S. Eidelman, A. Höcker and Z. Zhang, *Eur. Phys. J.* **C31**, 503–510 (2003).
31. SND Collaboration: M. N. Achasov *et al.*, *J. Exp. Theor. Phys.* **101**, 1053–1070 (2005).
32. W. J. Marciano and A. Sirlin, *Phys. Rev. Lett.* **61**, 1815–1818 (1988).
33. J. Erler, *Rev. Mex. Fis.* **50**, 200–202 (2004).
34. K. Maltman, *Phys. Lett.* **B633**, 512–518 (2006).
35. K. Melnikov and A. Vainshtein, *Phys. Rev.* **D70**, 113006 (2004).
36. M. Knecht and A. Nyffeler, *Phys. Rev.* **D65**, 073034 (2002).
37. M. Hayakawa and T. Kinoshita, eprint [hep-ph/0112102](#).
38. S. Davidson *et al.*, *JHEP* **0202**, 037 (2002).
39. NuTeV Collaboration: M. Goncharov *et al.*, *Phys. Rev.* **D64**, 112006 (2001).
40. A. D. Martin, R. G. Roberts, W. J. Stirling and R. S. Thorne, *Eur. Phys. J.* **C35**, 325–348 (2004).
41. G. A. Miller and A. W. Thomas, *Int. J. Mod. Phys.* **A20**, 95–98 (2005).
42. S. Kumano, *Phys. Rev.* **D66**, 111301 (2002).
43. A. B. Arbuzov, D. Y. Bardin and L. V. Kalinovskaya, *JHEP* **0506**, 078 (2005).
44. K. P. Diener, S. Dittmaier and W. Hollik, *Phys. Rev.* **D72**, 093002 (2005).
45. B. A. Dobrescu and R. K. Ellis, *Phys. Rev.* **D69**, 114014 (2004).
46. OPAL Collaboration: G. Abbiendi *et al.*, eprint [hep-ex/0601048](#).
47. H1 Collaboration: A. Specka *et al.*, eprint [hep-ex/0602007](#).
48. HPQCD and UKQCD Collaborations: Q. Mason *et al.*, *Phys. Rev. Lett.* **95**, 052002 (2005).
49. ALEPH, DELPHI, L3, and OPAL Collaborations and the LEP Working Group for Higgs Boson Searches: R. Barate *et al.*, *Phys. Lett.* **B565**, 61–75 (2003).
50. J. Erler, *Phys. Rev.* **D63**, 071301 (2001).
51. J. Erler and P. Langacker, *Phys. Lett.* **B456**, 68–76 (1999).
52. Qweak Collaboration: D. S. Armstrong *et al.*, *Eur. Phys. J.* **A24S2**, 155–158 (2005).
53. A. Czarnecki and W. J. Marciano, *Int. J. Mod. Phys.* **A15**, 2365–2376 (2000).
54. J. Erler, A. Kurylov and M. J. Ramsey-Musolf, *Phys. Rev.* **D68**, 016006 (2003).
55. J. Erler and M. J. Ramsey-Musolf, *Phys. Rev.* **D72**, 073003 (2005).
56. The Snowmass Working Group on Precision Electroweak Measurements: U. Baur *et al.*, eprint [hep-ph/0202001](#).
57. M. E. Peskin and T. Takeuchi, *Phys. Rev.* **D46**, 381–409 (1992).
58. M. J. G. Veltman, *Nucl. Phys.* **B123**, 89–99 (1977).
59. H. J. He, N. Polonsky and S. Su, *Phys. Rev.* **D64**, 053004 (2001).
60. V. A. Novikov, L. B. Okun, A. N. Rozanov and M. I. Vysotsky, *JETP Lett.* **76**, 127–130 (2002).